Supporting Information

Cold Atmospheric Plasma-Assisted Deposition of Ammonium Functionalized Glass Coating for Enhanced Antibacterial Properties

Venkat Kasi[a, b, #], Md Mahabubur Rahman[b, c, #], Akshay Krishnakumar[b, c, #], Ulisses Heredia Rivera[a, b], Devendra Sarnaik[a, b], Mithun Sinha[d], and Rahim Rahimi[a, b*]

[a]School of Materials Engineering, Purdue University, West Lafayette, IN 47907, USA.
[b]Birck Nanotechnology Center, Purdue University, West Lafayette, IN 47907, USA.
[c]School of Electrical and Computer Engineering, Purdue University, West Lafayette, IN 47907, USA.
[d] Division of Plastic Surgery, Department of Surgery, Indiana University School of Medicine, Indianapolis, IN 46202, USA

*Corresponding author email: rrahimi@purdue.edu
[#]Authors contributed equally to the manuscript

Keywords: Silica coating, Cold Atmospheric Plasma, Antibacterial Surfaces, Functionalized Ammonium   Compound
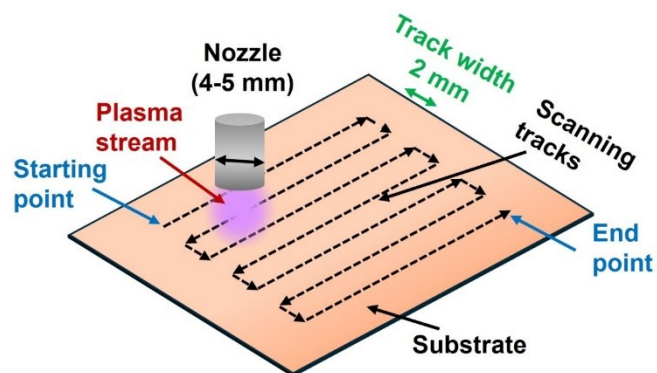
Figure S1: Schematic illustration of AF-SiO$_x$ coatings deposition pattern using cold atmospheric plasma assisted deposition technique.
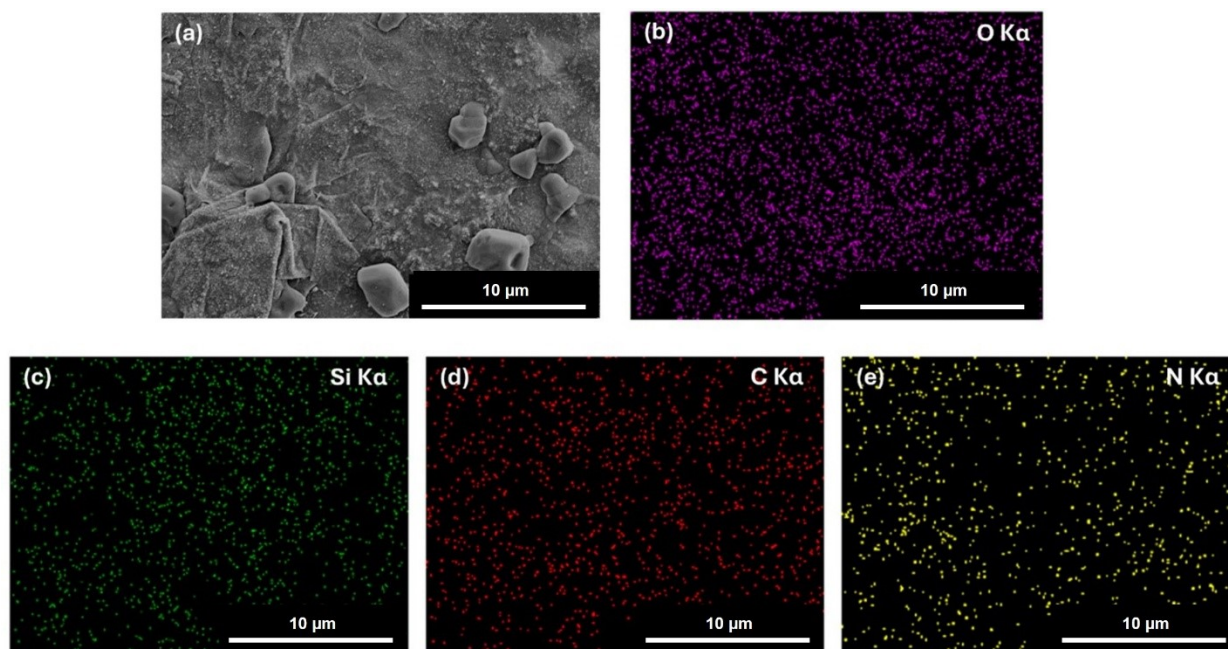

Figure S2. (a) High magnification SEM image of silica coating prepared with 1.0 wt% APS in the precursor mixture and EDX mapping for (b) O Kα, (c) Si Kα, (d) C Kα, and (e) N Kα for the same image.
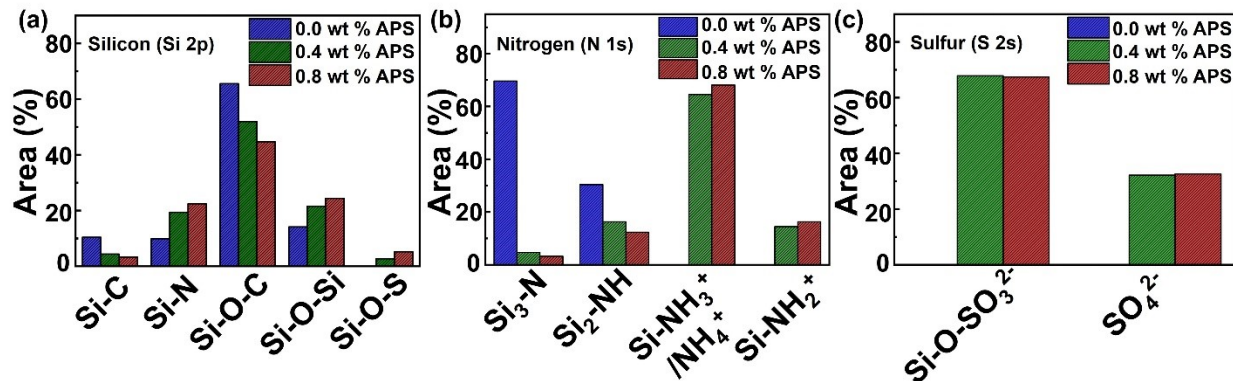
Figure S3: Deconvoluted high-resolution narrow scan spectra analysis for the coatings prepared with varying APS concentrations (0 wt%, 0.4 wt% and 0.8 wt%) in the precursor mixture. The area percentages of (a) Si 2p species (Si-C, Si-O-C, Si-O-Si , Si-N, Si-O-S), (b) N 1s species (Si$_3$-N, Si-NH$_3^+$/NH$_4^+$, Si-NH$_2^+$, Si$_2$-NH), and (c) S 2p species (Si-O-SO$_3^{2-}$, SO$_4^{2-}$) under the deconvoluted high-resolution XPS spectrum.
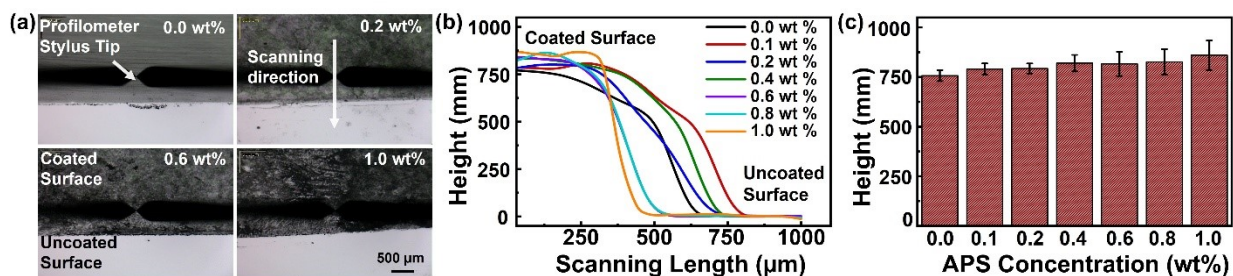
Figure S4: Thickness measurement of the AF-SiO$_x$ coatings prepared with varying concentrations of APS in the precursor mixture ranging from 0 to 1wt%. (a) Transverse scanning line and the direction of the profilometer stylus on the AF-SiO$_x$ coated samples, (b) Step profile line of profilometer measured on the AF-SiO$_x$ coated substrate, showing the difference in height between the coated and the uncoated area of the substrate, and (c) Average thickness of AF-SiO$_x$ coatings deposited with varying concentration of APS in the precursor mixture.
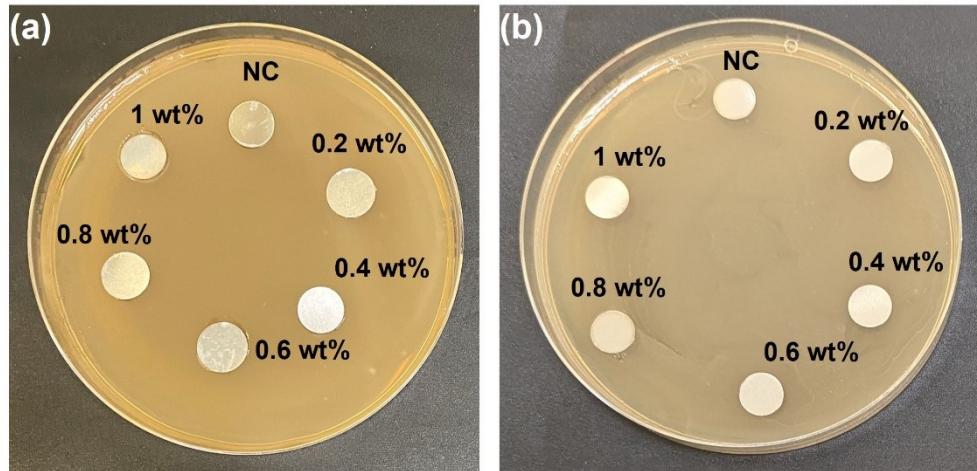
Figure S5: Inhibition zone analysis of CAP assisted AF-SiO$_x$ coated SS substrates with increasing concentration of APS concentration against (a) *E. coli* and (b) *S. aureus* bacterial populations. (NC: negative control, plain SS)
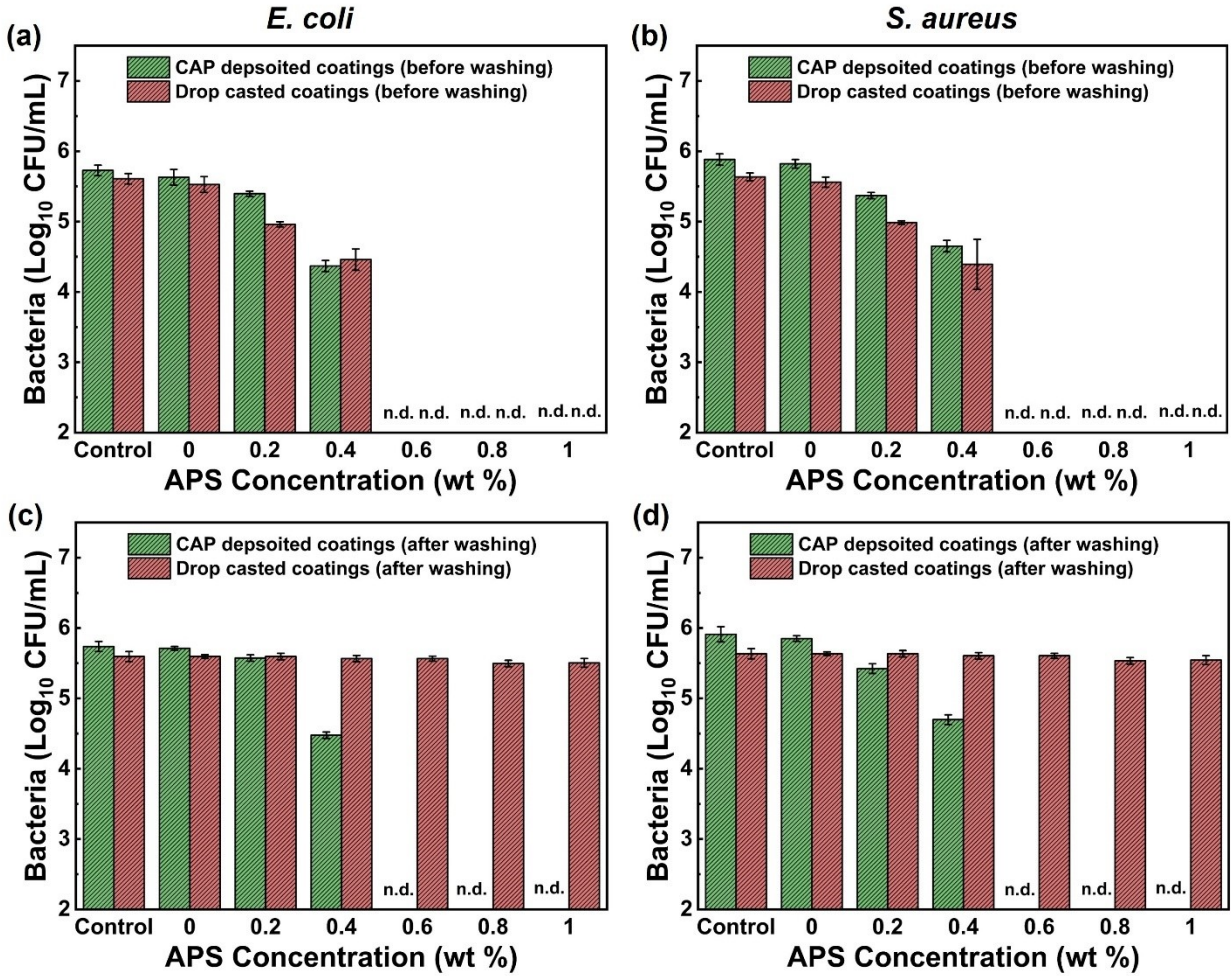
Figure S6: Antibacterial contact killing analysis of AF-SiO$_x$-coated SS substrates with varying APS concentrations in as-prepared and after incubation in simulated body fluid (SBF). Antibacterial property of the drop casted and CAP assisted AF-SiO$_x$ coating with various APS concentration before washing in SBF against (a) *E. coli*, (b) *S. aureus*, and drop-casted and CAP assisted SiO$_x$ coating with various APS concentration after washing in SBF against (c) *E. coli*, and (d) *S. aureus*.

Table S1: Atomic weight percentage of different species (C, O, N, Si and S) with varying concentration of APS in precursor mixture.

APS concentration (wt %)	Carbon (At %)	Oxygen (At %)	Nitrogen (At %)	Silicon (At %)	Sulfur (At %)
0	12.32	60.89	0.4	26.39	0
0.4	15.14	57.17	2.76	21.37	3.57
0.8	14.75	56.7	4.66	18.8	5.1